RESEARCH ARTICLE

Birds achieve high robustness in uneven terrain through active control of landing conditions

Aleksandra V. Birn-Jeffery* and Monica A. Daley

The Royal Veterinary College, Hawkshead Lane, North Mymms, Hatfield AL9 7TA, UK

*Author for correspondence (abirnjeffery@rvc.ac.uk)

SUMMARY

We understand little about how animals adjust locomotor behaviour to negotiate uneven terrain. The mechanical demands and constraints of such behaviours likely differ from uniform terrain locomotion. Here we investigated how common pheasants negotiate visible obstacles with heights from 10 to 50% of leg length. Our goal was to determine the neuro-mechanical strategies used to achieve robust stability, and address whether strategies vary with obstacle height. We found that control of landing conditions was crucial for minimising fluctuations in stance leg loading and work in uneven terrain. Variation in touchdown leg angle (θ_{TD}) was correlated with the orientation of ground force during stance, and the angle between the leg and body velocity vector at touchdown (β_{TD}) was correlated with net limb work. Pheasants actively targeted obstacles to control body velocity and leg posture at touchdown to achieve nearly steady dynamics on the obstacle step. In the approach step to an obstacle, the birds produced net positive limb work to launch themselves upward. On the obstacle, body dynamics were similar to uniform terrain. Pheasants also increased swing leg retraction velocity during obstacle negotiation, which we suggest is an active strategy to minimise fluctuations in peak force and leg posture in uneven terrain. Thus, pheasants appear to achieve robustly stable locomotion through a combination of path planning using visual feedback and active adjustment of leg swing dynamics to control landing conditions. We suggest that strategies for robust stability are context specific, depending on the quality of sensory feedback available, especially visual input.

Key words: robustness, uneven terrain, stability, load-dependent actuation.

Received 13 September 2011; Accepted 23 February 2012

INTRODUCTION

In natural environments, terrestrial animals regularly move over complex, uneven and unpredictable terrain. Negotiation of such environments involves unsteady locomotion, requiring changes in body velocity, body height or both from step to step. Unsteady behaviours likely produce different mechanical demands and constraints than steady locomotion (Biewener and Daley, 2007), and thus likely result in different selection pressures. Understanding the behavioural, neural and mechanical strategies used by animals for unsteady locomotion can provide insight into trade-offs among factors such as economy, dynamic stability and injury risk. Recent studies have used two main approaches to this topic: (1) theoretical analysis of dynamic stability characteristics, focusing on simplified models of body dynamics, often referred to as 'templates' (e.g. Full et al., 2002; Geyer et al., 2005; McGeer, 1990; Schmitt and Clark, 2009; Seipel and Holmes, 2007; Seipel et al., 2004; Seyfarth et al., 2003); and (2) experiments investigating how animals respond to specific terrain disturbances (Daley and Biewener, 2006; Farley et al., 1998; Ferris et al., 1998; Grimmer et al., 2008; Jindrich and Full, 2002; Marigold and Patla, 2005; Moritz and Farley, 2003; Sponberg and Full, 2008; Clark and Higham, 2011). Experimental approaches allow comparison of animal behaviour with model predictions, and can help identify whether proposed dynamic models adequately represent the neuro-mechanical control strategies used by animals.

The dynamics of steady, legged locomotion over uniform terrain can be described by a simple spring-loaded inverted pendulum model (SLIP) (e.g. Blickhan, 1989; Farley et al., 1993; Full and Koditschek, 1999; Geyer et al., 2006; McMahon and Cheng, 1990; Seipel and Holmes, 2007; Seyfarth et al., 2006; Seyfarth et al., 2002; Seyfarth et al., 2003). In this model, gravitational potential energy (E_P) and kinetic energy (E_K) are in phase and some energy is recovered through recoil in elastic structures (i.e. tendons) (Cavagna et al., 1977). During a step or stride cycle, the system is energy conservative, exhibiting no net changes in mechanical energy. The SLIP model describes only the overall body dynamics of locomotion, and is described as a neuro-mechanical 'template' (Full and Koditschek, 1999). Templates do not provide detailed knowledge of the complex underlying neuromuscular mechanisms, but may simplify control by acting as a target of the neuromuscular system (Daley and Biewener, 2006; Full and Koditschek, 1999). Neuro-mechanical templates have highlighted large-scale dynamic similarities across a diverse range of terrestrial animals (Farley et al., 1993; Full and Koditschek, 1999).

Animals can use a number of simple strategies to stabilise unsteady locomotion around the SLIP template. A gait is dynamically stable if the body returns to a periodic trajectory following a disturbance, and robustly stable if it can do so for large disturbances. Stability refers to whether the system recovers, and robustness to the maximum disturbance a system can recover from. When humans encounter surfaces of changing compliance or terrain height, they adjust leg stiffness (k_{leg}) and leg contact angle (θ_{TD}) to maintain a stable centre of mass (CoM) trajectory (Austin et al.,

1999; Farley et al., 1998; Ferris and Farley, 1997; Ferris et al., 1999; Ferris et al., 1998; Grimmer et al., 2008). These adjustments in leg parameters use simple feed-forward control mechanisms combined with passive dynamics to achieve stability. Leg retraction (backward motion of the leg relative to the body) in late swing phase results in an automatic adjustment of θ_{TD}, improving stability and robustness (Seyfarth et al., 2003). Empirical evidence shows that both humans and birds adjust θ_{TD} through leg retraction in the late swing phase (Blum et al., 2010; Daley and Biewener, 2006; Seyfarth et al., 2003).

Animals sometimes produce or absorb net energy during the recovery from a perturbation, which deviates from the SLIP template (e.g. Daley and Biewener, 2006; Daley et al., 2006). Alternative dynamic templates that include actuation have been proposed (Schmitt and Clark, 2009; Seipel and Holmes, 2007), but little experimental evidence exists to support one alternative template over another. Discovery of dynamic templates for unsteady locomotion would provide insights into mechanisms for robust stability in varied terrain, and could inspire novel control methods and mechanical designs for prosthetics and legged robots (Andrews et al., 2011; Grizzle et al., 2009).

It is likely that animals adjust their neuro-mechanical control strategies and target movement trajectory depending on context. Important contextual factors include whether the perturbation is anticipated (e.g. Daley et al., 2006; Ferris et al., 1999; Moritz and Farley, 2004) and whether visual feedback is involved (Patla, 1997; Patla et al., 1989; Wilkie et al., 2010). Anticipation and visual route planning may allow animals to adjust limb trajectories and body dynamics in a feed-forward manner, rather than relying on reflex responses to the perturbation. Thus, we expect anticipation to strongly influence how animals negotiate uneven terrain.

In this study, we investigated how common pheasants (*Phasianus colchicus*) adjust their leg and body dynamics to negotiate obstacles. We compared five obstacle terrain conditions with uniform terrain. Each obstacle terrain contained visible obstacles of a fixed height, ranging from 10 to 50% of leg length. Our goals were to: (1) investigate strategies for robust stability in uneven terrain and (2) test whether birds change their strategies with increasing terrain 'roughness'. We expected that pheasants would preserve conservative SLIP dynamics and rely on passive-dynamic stabilising mechanisms for small obstacles, but actively adjust their body movement trajectory and mechanical energy in anticipation of large obstacles. Previous studies have suggested that landing conditions (body velocity, leg angle and leg length at the beginning of stance) play a crucial role in the force and work during stance following terrain perturbations (Daley and Biewener, 2006; Müller et al., 2010). Consequently, we expected that the birds would actively alter these landing conditions to control stance dynamics in anticipation of obstacles.

MATERIALS AND METHODS
Animals
Six adult male common pheasants, *Phasianus colchicus* Linnaeus 1758, with body mass of 1.27±0.12 kg (mean ± s.d.) and standing hip height of 0.22±0.07 m, were obtained from a local breeder. We clipped the primary wing feathers to prevent flight. The Royal Veterinary College approved all procedures. The pheasants were trained to run steadily on a runway and treadmill.

Experimental procedure
The birds ran across a 5.4 m runway, consisting of five Kistler force plates (0.6×0.9 m; model 9287B, Hook, Hampshire, UK) sampling at 500 Hz. Plexiglas® surrounded the runway, supported by wooden boards (Fig. 1C). We placed markers on the pheasants for kinematic data collection (Fig. 1A). Birds were motivated using loud noises to run both ways across the runway into small black boxes placed at either end. We recorded kinematics at 250 Hz using eight Qualisys cameras (Gothenburg, Sweden) placed evenly around the experimental field. Force plates and Qualisys cameras were triggered synchronously. Force plate data were automatically filtered using a low-pass filter of 100 Hz. We varied obstacle heights between 0 (control trials) and 0.5 leg length (L_{leg}) by increments of $0.1L_{leg}$. Three individuals encountered the conditions in sequence from small to large obstacle terrain, and three encountered them in the reverse sequence. Two obstacles of equal height were placed on the runway, with approximately five steps between them (Fig. 1C). We identified steps across the runway with respect to the obstacles (Fig. 1C), with the 'on' obstacle step defined as step '0'.

Data analysis and measurements
We completed all data analysis in a custom-written script in MATLAB (release R2007b, The Mathworks Inc., Natick, MA, USA). Qualisys data were smoothed and interpolated to 500 Hz using a quintic spline with tolerances between 6.9×10^{-6} and 2.3×10^{-3} mm. Spline tolerances were calculated by taking the root mean square error of the Qualisys tracking residuals per camera for each trial. We used the average of the cranial and caudal markers to define an initial estimate of body CoM position, and the average tarsometatarsalphalangeal joint and toe markers to define foot position.

CoM velocity and position over time were calculated through single and double integration of acceleration data from the force plates, respectively. We derived initial velocity from kinematics using the path-match optimisation technique (Daley et al., 2006). Further to this method, because of potential CoM positional offset from marker placement on the back, we used a minimal-pitch optimisation to adjust the initial CoM position. We assumed that on average, during steady, uniform terrain locomotion, animals minimise torques during stance and avoid imparting pitch angular momentum, thus approximating a point-mass model. For each individual bird, we calculated the vertical and fore–aft shift required to minimise torque during steady locomotion. We assumed that our back marker placement was correctly centred on the midline of the body, and we constrained the optimised CoM position to be within the confines of a sagittal planar projection of the body. For each bird, we corrected the initial position for all trials based on the CoM positional offsets calculated from the uniform terrain trials. We then analysed the data by step cycles, defined from begin stance to begin stance of the contralateral leg (Fig. 1B).

Measures of body dynamics
The total mechanical energy of the body CoM (E_{CoM}) was calculated from the force-plate-derived position and velocity data:

$$E_{CoM} = E_K + E_P, \tag{1}$$

$$E_{CoM} = \tfrac{1}{2}m\mathbf{V}^2 + mgh , \tag{2}$$

where m is body mass, $\mathbf{g}$ is gravitational acceleration ($-9.81\,\mathrm{m\,s^{-2}}$), $\mathbf{V}$ is velocity and h is the vertical height of the CoM. Net changes in energies (E_{CoM}, E_P and E_K) were calculated between the start and end of each step cycle. We also calculated the total CoM power ($\mathbf{P}_{total}$) by summing the powers of component directions (velocity $\times$ ground reaction force). The total absolute CoM work ($|W_{total}|$) was calculated by integrating $\mathbf{P}_{total}$ after taking the absolute value.
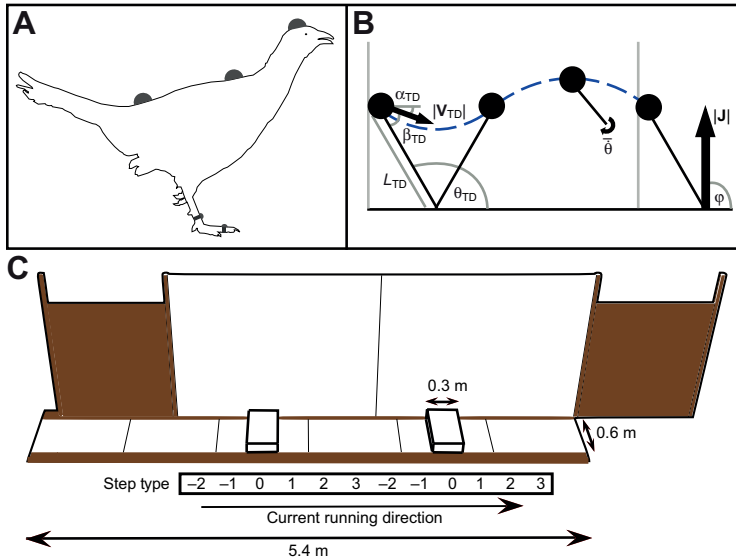
Fig. 1. Schematic depiction of the experimental setup. Force plate and kinematic data were collected in a runway. (A) Seven markers were positioned on the bird to allow estimation of leg length, leg angle, body centre of mass (CoM), position and velocity. We used initial position and velocity to calculate body dynamics (see the Materials and methods). Data were analysed by step cycle, as depicted by the vertical grey lines in B. A step cycle starts at a begin stance event [touchdown (TD)] and ends at TD of the contralateral leg. We measured leg angle (θ_{TD}), leg length (L_{TD}) and the velocity vector ($|\mathbf{V}_{TD}|$ and α_{TD}), and the angle between the leg and the velocity vector (β_{TD}) at TD. We also measured leg retraction velocity during late swing phase ($\bar{\dot{\theta}}$), the total sagittal impulse magnitude during stance ($|\mathbf{J}|$) and the associated impulse angle (φ). Steps were numbered sequentially relative to the obstacles (C).

From the ground reaction forces (**F**), we calculated the average vertical force ($\bar{F}_v$), net fore–aft force ($\hat{F}_{fa}$) and mean absolute fore–aft force ($|\bar{F}_{fa}|$). We also integrated the vertical and fore–aft forces over time to obtain the sagittal ground reaction force impulse (**J**), and calculated the impulse magnitude ($|\mathbf{J}|$) and angle (φ) over stance (Daley et al., 2006).

Finally, we calculated the axial and torsional work of the virtual leg. Here we define axial work as occurring through lengthening and shortening along the long axis of the virtual leg (the line connecting the body CoM to the toe). Net axial work ($\hat{W}_{axial}$) was found by:

$$P_{axial} = F_{axial} \cdot \dot{L}, \tag{3}$$

$$\hat{W}_{axial} = \int_t P_{axial}, \tag{4}$$

where P_{axial} is axial power, F_{axial} is axial force, $\dot{L}$ is leg length change and t is time. Torsional work is the work done through angular displacement by a force acting perpendicular to the line of the virtual leg ($F_\perp$). This involves a moment (M) tending to rotate the body about the CoM in the sagittal plane (pitching). Torsional work can provide insight into whether the birds deviate from the SLIP model, which assumes zero torques. Net torsional work ($\hat{W}_{tors}$) was calculated by:

$$M = F_\perp \cdot L, \tag{5}$$

$$P_{tors} = M \cdot \dot{\theta}, \tag{6}$$

$$\hat{W}_{tors} = \int_t P_{tors}, \tag{7}$$

where L is the effective virtual leg length, P_{tors} is torsional power and $\dot{\theta}$ is the leg retraction velocity.

Landing conditions and leg parameters

Previous work on unsteady locomotion highlights the strong relationship between landing conditions and the subsequent dynamics during stance (Daley and Biewener, 2006). Landing conditions refer to the state of the body and leg (position and velocity) at the time of touchdown (TD), marking the transition from swing to stance. We measured a number of landing conditions (Fig. 1B), including leg angle (θ_{TD}), leg length (L_{TD}) and body

velocity from the CoM velocity curves. Landing velocity magnitude ($|\mathbf{V}_{TD}|$) and angle (α_{TD}) were then calculated by:

$$\left|\mathbf{V}_{TD}\right| = \sqrt{\left(V_{faTD}\right)^2 + \left(V_{vTD}\right)^2} \tag{8}$$

and

$$\alpha_{TD} = \text{atan2}\,(V_{faTD}, V_{vTD}), \tag{9}$$

where V_{faTD} and V_{vTD} are the fore–aft and vertical velocity, respectively.

Lastly, we calculated the angle between the leg and the body velocity vector:

$$\beta_{TD} = (180 - \theta_{TD}) + \alpha_{TD}. \tag{10}$$

In addition to landing conditions, we measured two further leg parameters: the mean retraction velocity of the leg in late swing phase ($\bar{\dot{\theta}}$) and leg stiffness during stance (k_{leg}). Leg stiffness was estimated using two different methods: the first follows McMahon and Cheng (McMahon and Cheng, 1990) and assumes a steady mass-spring model; the second is the average stiffness only over the duration of leg compression (positive force increments with leg shortening) (Daley and Biewener, 2006). The latter method is better suited to unsteady data, as the timings of maximum compression and maximum force are not simultaneous. If the data exactly matched a passive SLIP model with a linear leg spring, the two k_{leg} values would be identical.

Selecting steady trials

It is not possible to control velocity in freely moving animals, and animals often accelerate and decelerate when moving overground. To focus our analysis on the effects of the obstacles, we aimed to minimise variance associated with acceleration. Firstly, we collected trials that appeared steady to the human eye, in which the bird ran forward in a straight line. Post-processing, we analysed the distribution of the fore–aft impulses across all uniform terrain trials to create values for classification of 'steady' and 'unsteady' trials. A perfectly steady step cycle has equal negative and positive fore–aft impulses, resulting in zero net fore–aft acceleration. We categorised as 'steady' any step with a net fore–aft impulse within ±1 s.d. of uniform terrain trials. This amounted to a maximum 10% increase or decrease in forward velocity. We included the uniform terrain steps within this range in
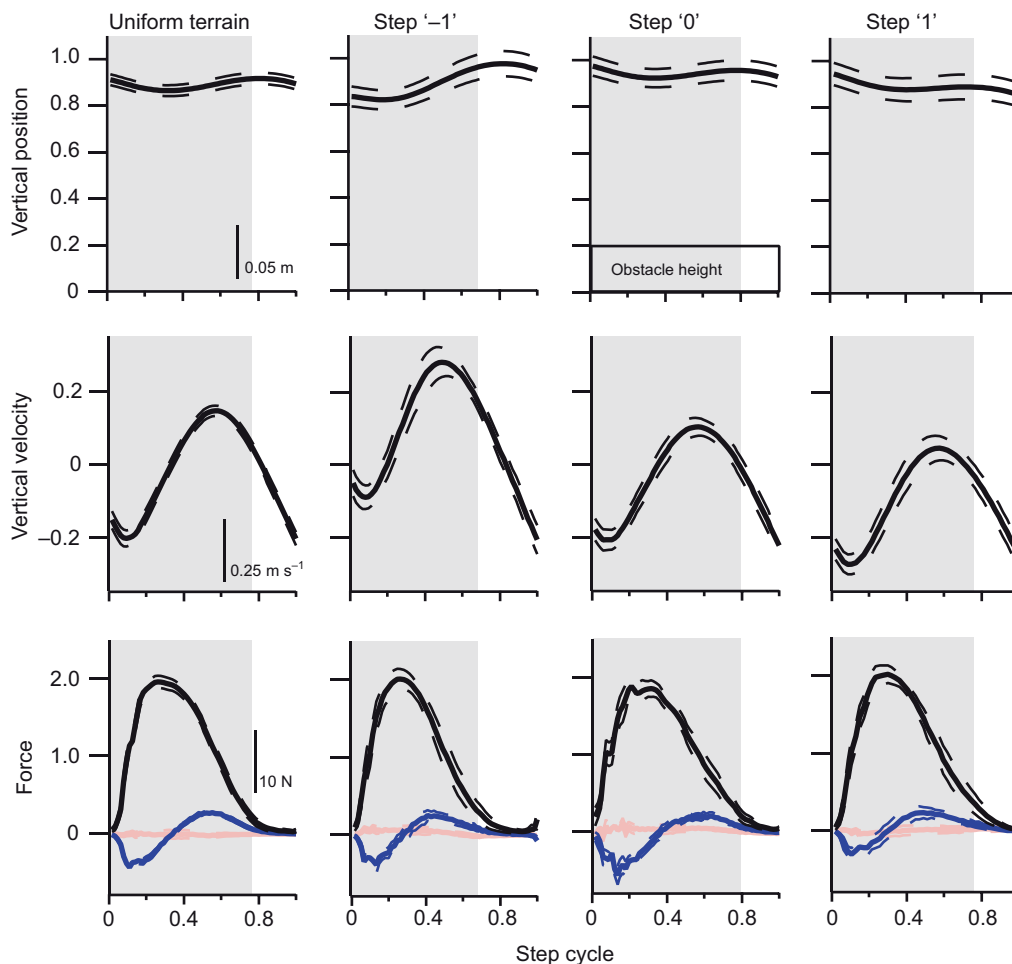
Fig. 2. Average vertical body CoM trajectories (position and velocity) and average ground reaction forces for uniform terrain and 0.2L_{leg} obstacle trials (steps '–1', '0' and '1'). Dashed lines indicate 95% confidence intervals. In the force plot, black denotes vertical force (F_v), blue denotes fore–aft force (F_{fa}) and pink denotes mediolateral force (F_{ml}). The grey boxes indicate the approximate stance phase. Variation increases between uniform terrain and all 0.2L_{leg} obstacle terrain. Peak vertical forces remain similar across terrain conditions.

the analysis as the control comparison. For obstacle trials, we categorised the 'approach' to the obstacle as steady or unsteady based on step '–2', and excluded trials with unsteady approaches from the analysis. This meant that the bird was steady before encountering the obstacle, but did not exclude potential 'unsteady' strategies for negotiating the obstacle itself. The mean velocity in uniform terrain trials was 2.57 m s^{-1} (range: 1.30–3.79 m s^{-1}) and in obstacle terrain, it was 2.60 m s^{-1} (range: 1.30–4.62 m s^{-1}).

Statistical analysis

The data analysed include 165 trials with a total of 441 step cycles. We obtained the following sample size within step categories: uniform terrain (control)=58, step '–1'=131, step '0'=141 and step '1'=111 (pooling across obstacle heights). To minimise variation due to body size, all variables in the analysis were normalised to dimensionless quantities using a combination of m, g and L_{leg} (e.g. McMahon and Cheng, 1990). All values reported in figures, tables and text are normalised dimensionless quantities (without units), unless otherwise specified.

ANOVAs were performed in MATLAB and *post hoc* analyses in SPSS (for Windows, release 17.0.1 2008, SPSS Inc., Chicago, IL, USA) after confirming that the data were normally distributed. All statistical analyses used an alpha level of 0.05. We performed two-way ANOVA, with individual as a random effect and step category as a fixed effect, and the data set split by obstacle height. We made *post hoc* comparisons of obstacle step categories to uniform terrain using unpaired *t*-tests (corrected for unequal variances where necessary), followed by sequential Bonferroni

corrections for multiple tests (Holm, 1979; Rice, 1989). Before *post hoc* comparisons, we corrected for individual as a factor based on each individual's difference from the grand mean in uniform terrain. Values reported in the text and figures are dimensionless means ± s.d., unless otherwise stated.

We used a regression analysis (Sokal and Rohlf, 1995) to investigate the effect of landing conditions and leg parameters on body CoM dynamics, with a pooled analysis and a separate analysis for each step category. We used a backward stepping procedure that minimised multi-collinearity and excluded non-significant variables using a custom-written script in MATLAB using the Statistics toolbox.

RESULTS
Variation in running dynamics over obstacle terrain

Compared with uniform terrain trials, we observed higher variability in body mechanics and leg posture in obstacle terrain (Fig. 2). The mean time course of vertical ground reaction forces remained similar across terrains, but the 95% confidence intervals increased, especially in the latter half of stance (Fig. 2). Similarly, we saw an increase in standard deviation across most variables in obstacle terrain (Table 1). Only two variables exhibited low variance in obstacle terrain: mean leg retraction velocity ($\bar{\theta}$; Table 1) and touchdown velocity angle (α_{TD}).

Variation in net change in total energy (ΔE_{CoM}) also increased in obstacle terrain, with significant shifts among obstacle step categories (Fig. 3, Table 1). All terrains exhibited a normal distribution in ΔE_{CoM} (Kolmogorov–Smirnov: uniform terrain, $P=0.2$; obstacle terrains,

Table 1. ANOVA results testing for differences among step type categories using sequential Bonferroni *post hoc* correction

Variable	Control mean	Obstacle height (% L_{leg})	P	Step type mean – control mean		
				Step '–1'	Step '0'	Step '1'
θ_{TD}	125.35±3.67	0.1	0.002	–2.02±5.83	0.92±7.28	–4.42±6.49*
		0.2	<0.001[†]	–1.06±7.29	3.01±6.67	–5.27±5.79*
		0.3	<0.001[†]	2.32±6.49	5.07±6.50*	–7.38±7.33*
		0.4	<0.001[†]	–1.65±5.96	5.89±6.18*	–9.02±4.31*
		0.5	<0.001[†]	–0.46±8.64	6.35±6.51*	–11.54±5.11*
β	50.50±4.95	0.1	0.001[†]	4.26±6.14*	–2.49±8.53	3.40±8.80
		0.2	<0.001[†]	4.09±8.65	–4.19±7.28*	2.62±7.19
		0.3	<0.001[†]	0.21±7.92	–5.24±7.07*	2.16±8.31
		0.4	<0.001[†]	5.27±8.29*	–6.60±7.89*	3.92±6.84
		0.5	<0.001[†]	7.43±10.62*	–6.59±6.88*	5.96±6.78*
ΔE_{CoM}	–0.02±0.08	0.2	<0.001	0.19±0.21*	–0.09±0.17*	0.02±0.24
		0.3	<0.001	0.21±0.25*	–0.07±0.24	0.07±0.19
		0.4	<0.001	0.30±0.22*	–0.10±0.28	0.03±0.17
		0.5	<0.001	0.39±0.20*	–0.09±0.16*	0.09±0.16*
φ	90.14±2.27	0.1	0.008	–1.48±5.84	–0.43±6.09	–4.27±6.00*
		0.3	<0.001	–1.03±5.63	2.22±6.88	–5.66±4.57*
		0.4	<0.001[†]	–1.84±4.47	2.59±6.43	–5.84±4.60*
		0.5	<0.001	–1.38±4.05	1.90±4.46	–9.19±5.42*
$\bar{\theta}$	37.09±11.65	0.2	<0.001[†]	2.83±13.89	7.97±11.75*	0.02±12.10
		0.4	<0.001[†]	8.99±13.81*	14.80±12.72*	0.76±11.25
		0.5	<0.001[†]	9.19±14.27*	17.96±13.65*	4.30±17.21

Table includes the variables with consistent significant changes in obstacle terrains. We report means ± s.d. for uniform terrain, and the mean differences from uniform terrain ± s.d. for obstacle terrains. *Significantly different from control; [†]variables where individual was a significant factor. See List of symbols and abbreviations for variable definitions.

P=0.098); however, the obstacle terrain showed some kurtosis with increasing data in the tails of the distribution (Fig. 3). In the approach step ('–1'), the distribution was shifted to the right, and all terrains above $0.1L_{leg}$ exhibited significant positive ΔE_{CoM} (Table 1). On the obstacle ('0'), heights $0.2L_{leg}$ and $0.5L_{leg}$ differed significantly from uniform terrain, with a small net negative ΔE_{CoM} (Fig. 3, Table 1).

Differences in body and leg dynamics among obstacle terrain step categories

To further investigate the strategies used to negotiate obstacles, we compared aspects of body dynamics, leg parameters and landing conditions among step categories in obstacle terrain (Table 1, Fig. 4).

In the approach step ('–1') the birds began stance with a shorter touchdown leg length (L_{TD}) and a more horizontally orientated velocity angle (α_{TD}; Fig. 4). During stance, net axial limb work ($\hat{W}_{axial}$) increased by up to +$0.33mgL_{leg}$ (uniform terrain: –0.16±0.09 J; maximum at $0.5L_{leg}$ obstacle terrain: 0.73±0.14 J), indicating leg actuation. This is associated with increased take-off leg length (L_{TO}: F_{183}=4.93, P<0.005; uniform terrain: 1.06±0.01; maximum at $0.4L_{leg}$ obstacle terrain: 1.18±0.02). Take-off velocity angle increased relative to uniform terrain (α_{TO}: F_{183}=6.19; P<0.005), but the mean vertical force ($\bar{F}_v$) and vertical impulse remained similar to the control (P>0.05). This indicates that the change in vertical velocity during stance remains similar to uniform terrain, and the higher take-off velocity relates to the increased velocity at touchdown (see Fig. 2). Thus, in the approach step ('–1'), the birds adjust touchdown vertical velocity and actuate the leg to increase body height in anticipation of the obstacle.

On the obstacle step ('0'), the birds adopted a crouched posture (smaller hip-to-toe height), indicated by shorter L_{TD} (Fig. 4), and increased touchdown leg angle (θ_{TD}) from the right horizontal (Table 1). Absolute fore–aft forces ($|\bar{F}_{fa}|$) increased in step '0' (Table 1), but with no shift in net fore–aft forces ($\hat{F}_{fa}$). This indicates larger accelerating and decelerating impulses of equal magnitude, resulting in no net change in forward momentum. $\bar{F}_v$ decreased

slightly in the obstacle step, but only significantly so in $0.5L_{leg}$ terrain (uniform terrain: 0.94±0.12; $0.5L_{leg}$ obstacle terrain: 0.83±0.14). These findings suggest a more crouched, compliant leg during stance, but with a nearly steady trajectory within the obstacle step.

In the step down from the obstacle (step '1'), the birds contacted the ground with a smaller θ_{TD} (more vertically oriented; Table 1), L_{TD} re-extended to the uniform terrain mean and α_{TD} decreased (Fig. 4). These changes in landing conditions were associated with a shift in ground reaction force orientation during stance. Impulse angle (φ) shifted forward and $\hat{F}_{fa}$ increased, indicating a net forward acceleration. ΔE_{CoM} remained near zero (Table 1, step '1'), so the forward acceleration resulted from conversion of gravitational E_P to forward E_K.

The birds also adjusted their leg retraction velocity ($\bar{\theta}$) in the late swing phase among step categories (Table 1). In the approach ('–1') and obstacle ('0') steps, $\bar{\theta}$ of the contralateral (swing) leg increased significantly. In the step down, $\bar{\theta}$ returned to the uniform terrain mean. These changes indicate adjustment of leg retraction velocity in the swing phases leading to stance on the obstacle and stance coming down from the obstacle.

Changes with increasing obstacle height

We primarily observed differences among step categories rather than with increasing obstacle height (Fig. 4). For example, in steps '–1' and '0', L_{TD} decreased relative to uniform terrain, but with no clear linear trend with increasing obstacle height. One notable exception, however, was α_{TD}, which did show a correlation with obstacle height in steps '–1' and '1' (Fig. 4). Step '–1' exhibited a positive correlation between obstacle height and α_{TD}. Step '1' showed an opposite trend: α_{TD} decreased with increasing obstacle height. On the obstacle, α_{TD} remained near uniform terrain mean. Among all aspects of dynamics measured, α_{TD} appears to be the most consistently controlled with respect to terrain height. Overall, however, we observed no sudden, qualitative change in strategy with increasing obstacle height.
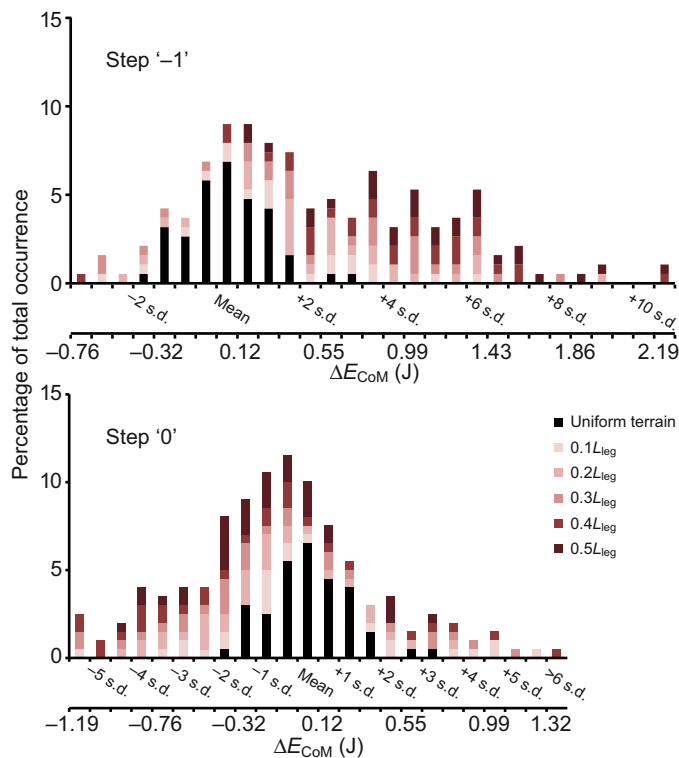
Fig. 3. Distribution of net change in mechanical energy of the body CoM (ΔE_{CoM}) in steps '–1' and '0' across terrain conditions. The distribution for uniform terrain is in black and obstacle trials are in shades of red (see key). Each horizontal bar represents 0.5 s.d. of the distribution over uniform terrain. The percentage of total occurrence is calculated from all steps across all terrain conditions within each step category. Distributions did not differ significantly from a normal distribution; however, the data are skewed positively in step '–1' and negatively in step '0'.

Influence of landing conditions on body dynamics

Although we did not observe many consistent trends with increasing obstacle height (other than α_{TD}, above), we noted substantially increased variation in body dynamics in obstacle terrain compared with uniform terrain (Table 1). We used regression analysis to investigate the relationships among body dynamics and landing conditions within this variation across trials.

The best overall predictors of body dynamics were θ_{TD} and the angle between the leg and the body velocity vector (β_{TD}). These landing condition variables predicted a large fraction of the trial-to-trial and step-to-step variance in axial and torsional limb work (Table 2, Fig. 5). θ_{TD} correlated with net torsional work ($\hat{W}_{tors}$; Table 2), whereas β_{TD} was a more consistent predictor of $\hat{W}_{axial}$ (Fig. 5), except for step '–1', during which θ_{TD} was a better predictor (Table 2). Changes in $\hat{W}_{axial}$ were larger than changes in $\hat{W}_{tors}$, such that $\hat{W}_{axial}$ was a good predictor of ΔE_{CoM} (Fig. 5). θ_{TD} also correlated with sagittal impulse angle (φ) across all step categories, with the best fit on step '0' (r_i^2=0.20–0.35; step '0' r_i^2=0.35). Thus, the touchdown variables β_{TD} and θ_{TD} predicted much of the variance in leg actuation, mechanical energy change and ground force orientation during stance across terrain types.

Among landing conditions, the velocity vector (α_{TD} and $|\mathbf{V}_{TD}|$) by itself did not consistently predict body dynamics. Velocity magnitude ($|\mathbf{V}_{TD}|$) did not vary across step categories or terrains, and the effect of α_{TD} was subsumed by the effect of β_{TD} (see schematic in Fig. 1B). In the regression models, β_{TD} predicted a larger fraction of the total variance than α_{TD} alone. Nonetheless,
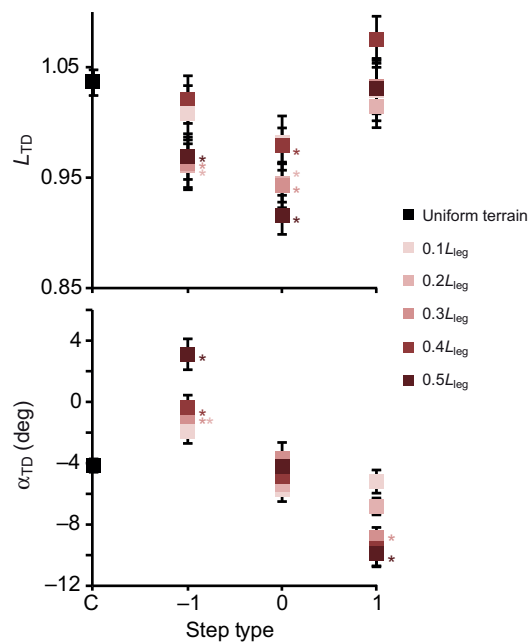

Fig. 4. Fractional effective leg length (L_{TD}) and velocity angle (α_{TD}) at touchdown across step categories for all terrain conditions. Error bars indicate ±s.e.m., revealing variation within terrain conditions, especially in L_{TD}. A consistent trend in α_{TD} is observed with increasing obstacle height in steps '–1' and '1'. C, control (uniform terrain). Asterisks denote significant differences to uniform terrain.

α_{TD} was an important component of β_{TD}, because it varied consistently with step category (Fig. 4). β_{TD} can vary from step to step depending on the interaction between α_{TD}, $\vec{\theta}$ and ground height.

Notably, neither of the two measures of leg stiffness (k_{leg}) emerged from the regression as a significant predictor of body dynamics during either obstacle or uniform terrain trials. Furthermore, k_{leg} did not differ significantly among step categories or obstacle heights in uneven terrain. The variance in k_{leg} was usually greater than the mean difference between terrain categories (uniform terrain: 19.43±13.51; $0.4L_{leg}$ 'on' obstacle terrain: 10.54±17.23).

Robust stability across obstacle terrain, but through an unsteady strategy

To analyse the overall sensitivity in body dynamics relative to the terrain 'roughness', we divided the birds' ΔE_P, ΔE_K and ΔE_{CoM} within each step by the energy change associated with the obstacle, $\Delta E_{P,obs}$ (as if change in body height was equal to the obstacle height: $mg\Delta H_{obs}$). Values closer to zero suggest lower sensitivity to the perturbation (Table 3). Across terrains and step categories, sensitivity was remarkably low, with most values below 0.25, and the highest value equal to 0.58. In steps '–1' and '0', fluctuations in E_P were larger than fluctuations in E_K. On the step down from the obstacle, E_K fluctuations were similar to E_P fluctuations. Sensitivity did not increase with obstacle height, but instead remained low even in the largest obstacle terrain.

In part, birds reduced sensitivity to the obstacles by adopting a crouched posture. If the pheasants crouched on step '0' with a reduction in hip height ($-\Delta H_{TD}$) equal to the obstacle height (diagonal line in Fig. 6), they could achieve a perfectly stable CoM trajectory with no change in CoM height on the obstacle. Hip height decreased significantly in obstacle steps (above $0.1L_{leg}$, F_{193}=11.65, P<0.005), but $-\Delta H_{TD}$ remained below 50% of the obstacle height.

Table 2. Regression analysis by step category, grouping obstacle terrain conditions

Dependent variable	Step type	P	Independent variable	b'	$r_{xi \cdot y}$	r_i^2	r^2 total
$\hat{W}_{axial}$	Uniform terrain	<0.005	β_{TD}	0.71	0.71	0.50	0.50
	−1	<0.005	θ_{TD}	−0.59	−0.51	0.30	0.49
	0	<0.005	β_{TD}	0.87	0.80	0.69	0.86
	1	<0.005	β_{TD}	0.82	0.72	0.59	0.71
	All steps	<0.005	β_{TD}	0.81	0.73	0.59	0.62
$\hat{W}_{tors}$	−1	<0.005	θ_{TD}	0.73	0.73	0.54	0.54
	0	<0.005	θ_{TD}	0.61	0.61	0.38	0.38
	1	<0.005	θ_{TD}	0.76	0.77	0.58	0.68
	All steps	<0.005	θ_{TD}	0.58	0.58	0.34	0.39

b', standardized coefficient; $r_{xi \cdot y}$, partial correlation; r_i^2, partial coefficient of determination (Sokal and Rohlf, 1995).
We included only significant factors with r_i^2 values greater than 0.15 (see Materials and methods). The best predictors of axial and torsional work ($\hat{W}_{axial}$ and $\hat{W}_{tors}$, respectively) across step categories were leg angle (θ_{TD}) and the angle between the leg and the body velocity vector (β_{TD}) at touchdown.

The birds did not maintain a perfectly steady trajectory over the obstacle, but did reduce sensitivity to the obstacle by crouching (up to 19% L_{leg})

Across obstacle terrains, the birds negotiated obstacles using the strategy illustrated in Fig. 7. The birds began step '−1' with a shallow velocity angle, and produced positive limb work during stance to increase body height before the obstacle. The positive ΔE_{CoM} during this step appeared as an increase in E_P at touchdown on the obstacle. The birds crouched and swept through a larger leg angle during stance on the obstacle (step '0'). Velocity remained relatively horizontal in step '0'. Stepping down from the obstacle (step '1'), the birds allowed their body to fall, resulting in a decrease in α_{TD} and a passive exchange of gravitational E_P to increase E_K. The take-off velocity vector (α_{TO}) was orientated horizontally, back to the uniform terrain mean.

DISCUSSION
Evidence of anticipation and active control
In this terrain environment, pheasants anticipate obstacles and likely use visual route planning to negotiate them. In the approach step ('−1'), the birds land with a higher velocity angle (Fig. 4) and produce net positive leg work during stance (Fig. 3), increasing hip height and vertical velocity at take-off (Fig. 2). The birds launch themselves

Fig. 5. Regression plots of β_{TD} against net axial work ($\hat{W}_{axial}$) across all terrains and step categories (A) and only the obstacle step, step '0' (B). Black lines indicate the best linear fit, and the grey dotted lines represent the 95% confidence intervals. The symbols in A represent step types (triangles, step '−1'; circles, step '0'; inverted triangles, step '1'). Colours are based on the net change in mechanical energy (ΔE_{CoM}): green indicates ΔE_{CoM} within two s.d. of the uniform terrain mean, red indicates positive ΔE_{CoM} and blue indicates negative ΔE_{CoM} more than two s.d. from the uniform terrain mean. β_{TD} is the most consistent predictor of body dynamics.

onto the obstacle, reducing changes in leg posture upon the obstacle. The positive work produced in the approach step increases with obstacle height (Table 3), suggesting that the birds visually gauge the obstacle height.

The above findings suggest that the birds target the obstacle. They adjust leg and body mechanics in anticipation of the obstacle, and achieve a relatively steady CoM trajectory within obstacle steps.

Although pheasants do anticipate obstacles and maintain a relatively steady trajectory within obstacle steps, they still land on obstacles with a more crouched posture than uniform terrain running (Fig. 6A). The anticipatory changes are not sufficient to completely avoid changes in landing conditions. Changes in terrain height cause the leg to contact the ground early or late. Previous studies have highlighted the important interactions between intrinsic mechanics and landing conditions for stable running (Daley and Biewener, 2006; Daley and Biewener, 2011; Daley et al., 2007; Grimmer et al., 2008; Müller and Blickhan, 2010). Postural changes at the time of ground contact are mediated through leg retraction and leg length change during the late swing phase (Blum et al., 2007; Blum et al., 2010; Seyfarth et al., 2003). Consequently, the swing leg trajectory is a crucial control target for stability, robustness and injury avoidance in uneven terrain (Blum et al., 2007; Blum et al., 2011; Daley and Usherwood, 2010; Seyfarth et al., 2003).

Pheasants appear to actively adjust swing leg retraction velocity to control landing conditions during obstacle negotiation. Swing leg retraction velocity increases in steps '−1' and '0', returning to the uniform terrain value immediately in the step down ('1'; Table 1). In the obstacle step, high retraction velocity in concert with increased body height avoids an excessively crouched posture on the obstacle. In the step down, high retraction velocity leads to lower robustness in terms of the normalised maximum drop in terrain, but it protects against excessive leg forces (Daley and Usherwood, 2010). We observed minimal change in vertical ground reaction forces across steps (Fig. 2). These findings suggest that the birds actively adjust leg retraction velocity to minimise fluctuations in ground reaction forces and leg posture, despite large variation in terrain height.

Is there a change in strategy with increasing terrain roughness?
We used several obstacle heights to understand whether birds change their strategies depending on obstacle size. We expected that the birds would maintain SLIP-like body dynamics in relatively uniform terrain (small obstacles), relying on passive-dynamic stabilising mechanisms, and would shift to non-conservative strategies for very rough terrain. Surprisingly, we did not observe an abrupt change in
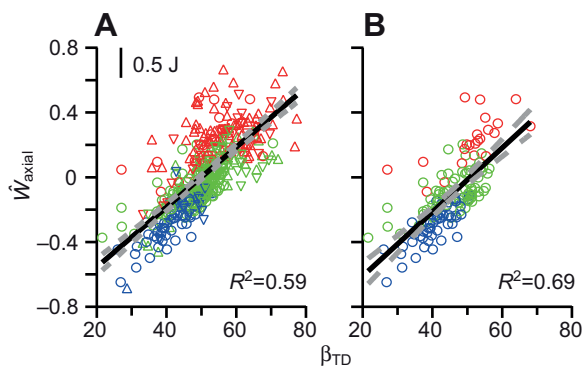
Table 3. Net changes in potential energy (E_P), kinetic energy (E_K) and total mechanical energy of the body centre of mass (E_{CoM}) for each step category, scaled relative to the obstacle height

			Step type mean	
	Obstacle height (fraction L_{leg})	Step '–1'	Step '0'	Step '1'
ΔE_P	0.1	0.25±0.05	–0.19±0.04	–0.28±0.04
	0.2	0.23±0.03	–0.10±0.02	–0.18±0.02
	0.3	0.24±0.02	–0.08±0.02	–0.19±0.02
	0.4	0.21±0.02	–0.09±0.02	–0.16±0.01
	0.5	0.26±0.03	–0.07±0.01	–0.15±0.01
ΔE_K	0.1	0.17±0.17	0.12±0.18	0.58±0.16
	0.2	0.12±0.06	–0.12±0.06	0.18±0.08
	0.3	0.02±0.06	–0.05±0.06	0.25±0.05
	0.4	0.09±0.03	–0.04±0.05	0.16±0.04
	0.5	0.04±0.02	–0.01±0.02	0.20±0.02
ΔE_{CoM}	0.1	0.42±0.17	–0.07±0.20	0.30±0.17
	0.2	0.35±0.08	–0.22±0.06	0±0.09
	0.3	0.26±0.06	–0.13±0.06	0.06±0.05
	0.4	0.30±0.04	–0.13±0.05	0±0.04
	0.5	0.30±0.03	–0.09±0.02	0.05±0.02

Values are means ± s.e.m. Values near zero suggest low sensitivity to the terrain perturbation (and higher robustness). Sensitivity is remarkably low, indicating that the birds achieve high robustness to variations in terrain height.

strategy. We observed two gradual shifts in strategy: (1) a plateau at 19% L_{leg} in the extent of 'crouching' on the obstacle, so a larger fraction of the obstacle height was overcome through changes in body CoM height for large obstacles; and (2) an increase in positive work in the approach step, consistent with the larger increase in CoM height to overcome larger obstacles.

Fig. 6. Fluctuations in hip height (A) at the beginning of stance on the obstacle compared with uniform terrain (ΔH_{TD}) and (B) during stance on the obstacle (ΔH_{stance}). If the birds minimise fluctuations in CoM height relative to the original ground height, they must crouch their leg to compensate for the obstacle (decreasing ΔH_{TD} with increasing obstacle height; diagonal line in A). Crouching is significant above 0.2L_{leg}; however, this accounts for <50% of the obstacle height for larger obstacles. On the obstacle, the birds maintain a similar height during stance, remaining relatively close to the horizontal line, representing zero net change in height (B). Asterisks denote significant differences to uniform terrain and error bars are ±s.e.m.

For example, for 0.2L_{leg} obstacles, a crouched posture accounts for 60% of the obstacle height, leaving 40% to be negotiated by increasing the CoM height. In contrast, for 0.5L_{leg} obstacles, only 40% is accounted by crouching, leaving 60% to be negotiated by increasing body height (Fig. 6).

Control of landing conditions

Landing conditions (leg posture and body velocity at the start of stance) are the best predictors of body dynamics throughout the obstacle terrains. Leg angle (θ_{TD}) and the angle between the leg and body velocity (β_{TD}) at touchdown correlate strongly with stance phase dynamics (Table 2, Fig. 5). Several previous studies noted the importance of landing posture for stance dynamics (Biewener and Daley, 2007; Daley et al., 2006; Daley et al., 2009; Müller et al., 2010), suggesting that these may be crucial factors in intrinsic mechanics and key control targets for the neuromuscular system.

Conceptually, β_{TD} is an important contact condition to control leg loading in a system that avoids large torques. At the beginning of stance, β_{TD} divides the momentum of the body between translational (directed along the leg axis) and rotational (directed about the foot point). β_{TD} defines an upper limit to axial leg loading according to impulse–momentum balance (Biewener and Daley, 2007; Daley and Biewener, 2006). An increase in β_{TD} is associated with reduced leg loading, faster angular sweep during stance and shorter stance duration. Leg loading approaches zero as β_{TD} approaches 90 deg. Birds running over an unexpected terrain drop exhibit this relationship between β_{TD} and leg loading (Daley and Biewener, 2006). Here, we observed this effect, with the additional strong correlation between β_{TD} and axial work (Fig. 5). Previous perturbation experiments have also observed posture-dependent actuation, relating to either leg length or hip height at touchdown (Daley and Biewener, 2006; Daley and Biewener, 2011; Daley et al., 2009). These findings highlight the dynamic interactions among landing posture, leg loading and leg actuation, particularly in unsteady locomotion.

Posture-dependent leg actuation likely arises from the interaction between leg loading and pre-activation of stance muscles. Because of delays in excitation–contraction coupling, pre-activation of stance muscles occurs approximately 30–70 ms before ground contact (Dietz et al., 1979; Engberg and Lundberg, 1969; Gorassini
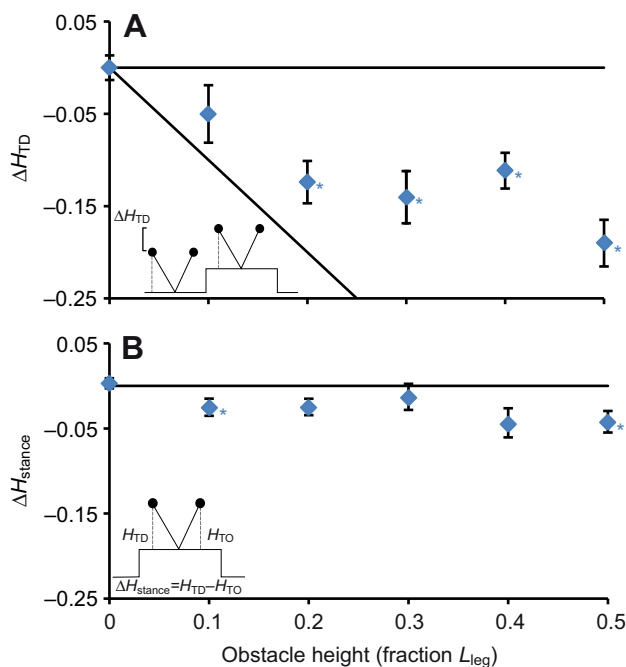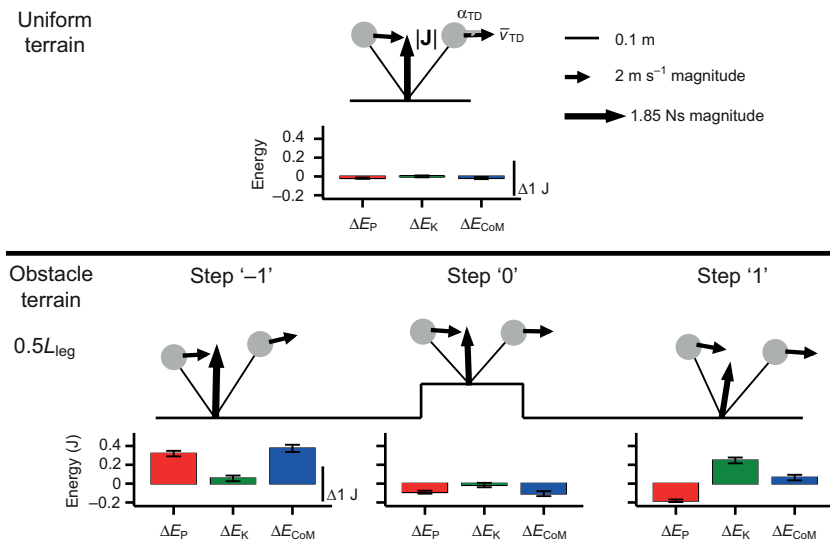
Fig. 7. Schematic representation of how pheasants negotiate obstacle terrain. The overall strategy remained similar across terrains. For clarity, we illustrate the largest obstacle condition ($0.5L_{leg}$). In the approach step ('−1'), the birds increase potential energy (E_P) through net positive work, resulting in a higher vertical position at touchdown on the obstacle. In the obstacle step ('0'), the birds' body CoM trajectory remains similar to that on uniform terrain. In the step down ('1'), E_P decreases and kinetic energy (E_K) increases with little change in total mechanical energy, suggesting passive energy exchange.

et al., 1994; Smith et al., 1993). Muscle activation level is set in a pre-determined feed-forward manner for the first ~30 ms of stance (Daley et al., 2009; Marigold and Patla, 2005; Moritz and Farley, 2004). Only beyond this time will feedback from proprioceptors lead to altered muscle contraction (for a review, see Duysens et al., 2000). Variation in leg loading will result in altered force–velocity and force–length muscle dynamics, and altered muscle work output (Daley and Biewener, 2011; Daley et al., 2009). Thus, control of force and work output of the limb requires careful control and appropriate adjustment of landing conditions through either active or passive-dynamic mechanisms.

Implications for simple models

Birds negotiate this uneven terrain environment using net changes in mechanical energy. A SLIP model is not sufficient to model this behaviour; it requires an actuated dynamic template. Actuated SLIP models, including either torsional 'hip' or linear 'leg' actuation, can improve stability and robustness in unsteady locomotion (Schmitt and Clark, 2009; Seipel and Holmes, 2007). Future work should test whether our data could be modelled well using a modified SLIP model with a linear leg actuator, and with work output dependent on β_{TD}. Controlling locomotion around an underlying dynamic template may simplify the complexity of neuromuscular control, whilst facilitating economy and robust stability (Daley and Biewener, 2006; Full and Koditschek, 1999).

Context-dependent locomotor control

Previous work in obstacle negotiation has shown that the primary response occurs on the obstacle, acting to stabilise the disturbed leg mechanics (Daley and Biewener, 2011). However, in the present study, the birds anticipated the obstacle, achieving a steady trajectory on the obstacle by significantly changing CoM and leg dynamics in the approach step and after the obstacle.

In the step down from the obstacle (step '−1'), we observed passive energy exchange between E_P and forward E_K, and changes in landing conditions similar to those seen in unexpected drop perturbation experiments (Daley et al., 2007; Daley et al., 2006). This strategy of using energy-conservative passive stabilisation is consistent with the SLIP model, and provides inherent stability in high-speed locomotion (Seyfarth et al., 2002).

The differences between this study and previous studies of unsteady locomotion in birds suggest that control strategies in uneven terrain are context specific (Daley and Biewener, 2006; Daley and Biewener, 2011; Daley et al., 2009). In the present study, the birds clearly anticipated and targeted the obstacle using active mechanisms. In contrast, birds relied primarily on passive-dynamic responses to negotiate unexpected terrain drops and low-contrast obstacles on a treadmill. The strategy used in the previous obstacle study may have been constrained by the nature of treadmill locomotion (Daley and Biewener, 2011). To maintain position on the treadmill belt, the birds must maintain relatively constant forward velocity, but overground velocity is less restricted. Velocity magnitude did not vary step-to-step in the obstacle terrain, but the birds adjusted velocity angle, re-directing velocity between vertical and fore–aft directions. We also cannot rule out the possibility that differences between this and previous studies relate to species-specific responses between guinea fowl and pheasants. Further studies of unsteady locomotion are required to fully understand how neuro-mechanical strategies vary depending on terrain, morphology and the quality and nature of sensory information available.

Species-dependent control strategies: birds *versus* humans

Birds allow large fluctuations in body trajectory upon encountering changes in terrain, whereas humans maintain a steady body trajectory by adjusting leg mechanics and landing conditions (Grimmer et al., 2008; Moritz and Farley, 2003). However, the differences between the results of studies in humans and birds may relate to the relative size of the terrain disturbance. For example, humans crouch on a step up to maintain constant vertical trajectory (Grimmer et al., 2008); however, the obstacles were no larger than $0.15L_{leg}$, which is small compared with pheasants running over $0.5L_{leg}$ obstacles in the present study. We do not know whether humans would maintain similar body motion by crouching at higher obstacle heights, but it is unlikely because of the high muscle forces and increased energy cost associated with a crouched posture (Biewener, 1989; Carrier et al., 1994; McMahon et al., 1987). We expect that humans and other large animals with upright posture are unlikely to adopt a significantly crouched posture to negotiate large obstacles, and would exhibit a larger shift in strategy than we observed in pheasants.

It appears that humans adjust k_{leg} to maintain dynamic stability, whereas birds use leg actuation and kinematic control strategies. Humans maintain a steady CoM trajectory in the face of substrate perturbations by adjusting k_{leg} (Farley et al., 1998; Ferris and Farley,

1997; Ferris et al., 1998; Moritz and Farley, 2004). A large range of k_{leg} values can be used to effectively run in a stable spring-like manner (Blum et al., 2011; Blum et al., 2010; Daley and Biewener, 2006; Daley et al., 2007; Seyfarth et al., 2003). Estimated k_{leg} varied widely in the pheasants in the present study, and did not correlate with stance dynamics, similar to a previous study of bird running (Daley and Biewener, 2006), suggesting either that k_{leg} is not an important variable and not controlled or that a linear estimate of leg stiffness is not appropriate for avian running. Because of their limb configuration, birds can use numerous kinematic strategies to stabilise running, whereas the straight-legged posture of humans limits the kinematic control strategies available to them (Blum et al., 2011).

Birds choose 'safety' over passive-dynamic stability

In previous perturbation experiments, birds demonstrated remarkable stability and robustness with little or no anticipatory preparation, using 'passive-dynamic' stabilising mechanisms (Daley and Biewener, 2006; Daley and Biewener, 2011; Daley et al., 2007; Daley et al., 2009). Why did the pheasants here use anticipatory strategies, even for small obstacles, if they could rely on passive stabilisation strategies? We suggest that animals often choose safety over passive stability when sufficient information exists about the terrain environment, minimising the likelihood of a catastrophic fall or injury. Humans also choose 'safety' over passive strategies in complex environments (Jansen et al., 2011). Birds may actively target obstacles to minimise the likelihood of an ill-placed footfall during high-speed locomotion, which could result in a broken leg or being eaten by a predator, for example.

A traditional measure of stability is minimisation of CoM fluctuations throughout a perturbation (Gatesy and Biewener, 1991; Leeuwen, 1999). During obstacle negotiation, however, minimising height fluctuations requires adopting a crouched posture. Crouched posture decreases effective mechanical advantage (Biewener, 1989) and requires that muscles operate at sub-optimal length and velocity. Although intrinsic changes in muscle force–length dynamics can be stabilising (Brown and Loeb, 2000; Daley et al., 2009; Jindrich and Full, 2002), they may cause muscles to contract less economically, and can also lead to muscle injury. Animals may reserve crouching strategies as a 'safety net' for truly unexpected perturbations. In the current obstacle negotiation task, the birds avoid extreme postures and prioritise constant velocity and ground forces rather than a steady CoM trajectory. These observations suggest that pheasants prioritise safety and economy over stability in the traditional sense (measured as a smooth CoM trajectory).

The role of vision in route planning for obstacle negotiation

Information on the roles of vision in controlling locomotion remains sparse. Successfully negotiating obstacles requires the use of both optic flow and feedback of current body motion to judge contact time (Martin, 2011; Pakan and Wylie, 2006), allowing route planning and preparation (Patla, 1997; Wilkie et al., 2010). In obstacle terrain, pheasants maintain constant velocity magnitude across step categories (Fig. 7), which may help achieve steady optical flow, facilitating depth perception (Davies and Green, 1988; Kral, 2003). Maintenance of constant velocity is likely to facilitate accurate path planning and robustly stable running in uneven terrain. Birds also have lower-field myopia (near-sightedness), allowing them to keep the ground in focus at eye height with the upper field focused at distances (Hodos and Erichsen, 1990; Schaeffel et al., 1994), enhancing their ability to dynamically gauge terrain. The results of the present study suggest that birds use visual route planning when presented with sufficient visual information. The interplay of visual and locomotor dynamics is likely to play a crucial role in the control of locomotion over uneven terrain.

Conclusions

Pheasants achieve robustly stable locomotion in uneven terrain through a combination of path planning using visual feedback and active adjustment of leg swing dynamics. These strategies control landing conditions to minimise fluctuations in leg forces and posture. The angle between the leg and velocity vector (β_{TD}) appears to be a crucial control target, due to its relationship with limb loading and net leg work during the consequent stance phase. The resulting leg actuation is inherently stabilising of body velocity and total mechanical energy in uneven terrain. A passive SLIP model will not suffice to model these data. The birds use a non-conservative strategy to negotiate obstacles, actuating the leg to launch onto the obstacle. We suggest that a modified SLIP model with a linear leg actuator is required to model bird locomotion.

LIST OF SYMBOLS AND ABBREVIATIONS

CoM	centre of mass of the body
E_{CoM}	total mechanical energy of the body CoM (sum of E_P and E_K)
E_K	kinetic energy of the CoM
E_P	gravitational potential energy of the CoM
F	ground reaction force
J	sagittal impulse
k_{leg}	leg stiffness
L	effective virtual leg length, measured between the CoM and the toe
L_{leg}	resting leg length measured as hip height during quiet standing
m	body mass
M	moment about the body CoM
P	power of the CoM
SLIP	spring-loaded inverted pendulum
V	velocity
W	work done on the CoM
ΔE_{CoM}	change in total energy of the CoM over a step cycle (implies net work done)
α	velocity angle
β	angle between the leg and body velocity vector
φ	sagittal impulse angle
θ	leg angle
$\dot{\theta}$	leg retraction velocity

REFERENCES

Andrews, B., Miller, B., Schmitt, J. and Clark, J. E. (2011). Running over unknown rough terrain with a one-legged planar robot. *Bioinspir. Biomim.* **6**, 026009.

Austin, G. P., Garrett, G. E. and Bohannon, R. W. (1999). Kinematic analysis of obstacle clearance during locomotion. *Gait Posture* **10**, 109-120.

Biewener, A. (1989). Scaling body support in mammals: limb posture and muscle mechanics. *Science* **245**, 45-48.

Biewener, A. A. and Daley, M. A. (2007). Unsteady locomotion: integrating muscle function with whole body dynamics and neuromuscular control. *J. Exp. Biol.* **210**, 2949-2960.

Blickhan, R. (1989). The spring-mass model for running and hopping. *J. Biomech.* **22**, 1217-1227.

Blum, Y., Rummel, J. and Seyfarth, A. (2007). Advanced swing leg control for stable locomotion. In *Autonome Mobile Systeme 2007* (ed. K. Berns and T. Luksch), pp. 301-307. Heidelberg: Springer-Verlag.

Blum, Y., Lipfert, S. W., Rummel, J. and Seyfarth, A. (2010). Swing leg control in human running. *Bioinspir. Biomim.* **5**, 026006.

Blum, Y., Birn-Jeffery, A., Daley, M. A. and Seyfarth, A. (2011). Does a crouched leg posture enhance running stability and robustness? *J. Theor. Biol.* **281**, 97-106.

Brown, I. E. and Loeb, G. E. (2000). A reductionist approach to creating and using neuromechanical models. In *Biomechanics and Neural Control of Posture and Movement* (ed. J. M. Winters and P. E. Crago), pp. 148-163. New York: Springer-Verlag.

Carrier, D. R., Heglund, N. C. and Earls, K. D. (1994). Variable gearing during locomotion in the human musculoskeletal system. *Science* **265**, 651-653.

Cavagna, G. A., Heglund, N. C. and Taylor, C. R. (1977). Mechanical work in terrestrial locomotion: two basic mechanisms for minimizing energy expenditure. *Am. J. Physiol. Regul. Integr. Comp. Physiol.* **233**, R243-R261.

Clark, A. J. and Higham, T. E. (2011) Slipping, sliding and stability: locomotor strategies for overcoming low-friction surfaces. *J. Exp. Biol.* **214**, 1369-1378.

Daley, M. A. and Biewener, A. A. (2006). Running over rough terrain reveals limb control for intrinsic stability. *Proc. Natl. Acad. Sci. USA* **103**, 15681-15686.

Daley, M. A. and Biewener, A. A. (2011). Leg muscles that mediate stability: mechanics and control of two distal extensor muscles during obstacle negotiation in the guinea fowl. *Philos. Trans. R. Soc. Lond. B* **366**, 1580-1591.

Daley, M. A. and Usherwood, J. R. (2010). Two explanations for the compliant running paradox: reduced work of bouncing viscera and increased stability in uneven terrain. *Biol. Lett.* **6**, 418-421.

Daley, M. A., Usherwood, J. R., Felix, G. and Biewener, A. A. (2006). Running over rough terrain: guinea fowl maintain dynamic stability despite a large unexpected change in substrate height. *J. Exp. Biol.* **209**, 171-187.

Daley, M. A., Felix, G. and Biewener, A. A. (2007). Running stability is enhanced by a proximo-distal gradient in joint neuromechanical control *J. Exp. Biol.* **210**, 383-394.

Daley, M. A., Voloshina, A. and Biewener, A. A. (2009). The role of intrinsic muscle mechanics in the neuromuscular control of stable running in the guinea fowl. *J. Physiol.* **587**, 2693-2707.

Davies, M. N. O. and Green, P. R. (1988). Head-bobbing during walking, running and flying: relative motion perception in the pigeon. *J. Exp. Biol.* **138**, 71-91.

Dietz, V., Schmidtbleicher, D. and Noth, J. (1979). Neuronal mechanisms of human locomotion. *J. Neurophysiol.* **42**, 1212-1222.

Duysens, J., Clarac, F. and Cruse, H. (2000). Load-regulating mechanisms in gait and posture: comparative aspects. *Physiol. Rev.* **80**, 83-133.

Engberg, I. and Lundberg, A. (1969). An electromyographic analysis of muscular activity in the hindlimb of the cat during unrestrained locomotion. *Acta Physiol. Scand.* **75**, 614-630.

Farley, C. T., Glasheen, J. and McMahon, T. A. (1993). Running springs: speed and animal size. *J. Exp. Biol.* **185**, 71-86.

Farley, C. T., Houdijk, H. H. P., Van Strien, C. and Louie, M. (1998). Mechanism of leg stiffness adjustment for hopping on surfaces of different stiffnesses. *J. Appl. Physiol.* **85**, 1044-1055.

Ferris, D. P. and Farley, C. T. (1997). Interaction of leg stiffness and surface stiffness during human hopping. *J. Appl. Physiol.* **82**, 15-22.

Ferris, D. P., Louie, M. and Farley, C. T. (1998). Running in the real world: adjusting leg stiffness for different surfaces. *Proc. R. Soc. Lond. B* **265**, 989-994.

Ferris, D. P., Liang, K. and Farley, C. T. (1999). Runners adjust leg stiffness for their first step on a new running surface. *J. Biomech.* **32**, 787-794.

Full, R. J. and Koditschek, D. E. (1999). Templates and anchors: neuromechanical hypotheses of legged locomotion on land. *J. Exp. Biol.* **202**, 3325-3332.

Full, R. J., Kubow, T., Schmitt, J., Holmes, P. and Koditschek, D. (2002). Quantifying dynamic stability and maneuverability in legged locomotion. *Integr. Comp. Biol.* **42**, 149-157.

Gatesy, S. M. and Biewener, A. A. (1991). Bipedal locomotion-effects of speed, size and limb posture in birds and humans. *J. Zool.* **224**, 127-147.

Geyer, H., Seyfarth, A. and Blickhan, R. (2005). Spring-mass running: simple approximate solution and application to gait stability. *J. Theor. Biol.* **232**, 315-328.

Geyer, H., Seyfarth, A. and Blickhan, R. (2006). Compliant leg behaviour explains basic dynamics of walking and running. *Proc. R. Soc. Lond. B* **273**, 2861-2867.

Gorassini, M. A., Prochazka, A., Hiebert, G. W. and Gauthier, M. J. (1994). Corrective responses to loss of ground support during walking. I. Intact cats. *J. Neurophysiol.* **71**, 603-610.

Grimmer, S., Ernst, M., Gunther, M. and Blickhan, R. (2008). Running on uneven ground: leg adjustment to vertical steps and self-stability. *J. Exp. Biol.* **211**, 2989-3000.

Grizzle, J. W., Hurst, J., Morris, B., Park, H. W. and Sreenath, K. (2009). MABEL, a new robotic bipedal walker and runner. In *Proceedings of the 2009 American Control Conference*, pp. 2030-2036. Piscataway, NJ: IEEE Press.

Hodos, W. and Erichsen, J. T. (1990). Lower-field myopia in birds: an adaptation that keeps the ground in focus. *Vision Res.* **30**, 653-657.

Holm, S. (1979). A simple sequentially rejective multiple test procedure. *Scand. J. Statist.* **6**, 65-70.

Jansen, S., Toet, A. and Werkhoven, P. (2011). Human locomotion through a multiple obstacle environment: strategy changes as a result of visual field limitation. *Exp. Brain Res.* **212**, 449-456.

Jindrich, D. L. and Full, R. J. (2002). Dynamic stabilization of rapid hexapedal locomotion. *J. Exp. Biol.* **205**, 2803-2823.

Kral, K. (2003). Behavioural-analytical studies of the role of head movements in depth perception in insects, birds and mammals. *Behav. Processes* **64**, 1-12.

Leeuwen, J. L. (1999). Neuromuscular control: introduction and overview. *Philos. Trans. R. Soc. Lond. B* **354**, 841-847.

Marigold, D. S. and Patla, A. E. (2005). Adapting locomotion to different surface compliances: neuromuscular responses and changes in movement dynamics. *J. Neurophysiol.* **94**, 1733-1750.

Martin, G. R. (2011). Understanding bird collisions with man-made objects: a sensory ecology approach. *Ibis* **153**, 239-254.

McGeer, T. (1990). Passive bipedal running. *Proc. R. Soc. Lond. B* **240**, 107-134.

McMahon, T. A. and Cheng, G. C. (1990). The mechanics of running: how does stiffness couple with speed? *J. Biomech.* **23 Suppl. 1**, 65-78.

McMahon, T. A., Valiant, G. and Frederick, E. C. (1987). Groucho running. *J. Appl. Physiol.* **62**, 2326-2337.

Moritz, C. T. and Farley, C. T. (2003). Human hopping on damped surfaces: strategies for adjusting leg mechanics. *Proc. R. Soc. Lond. B* **270**, 1741-1746.

Moritz, C. T. and Farley, C. T. (2004). Passive dynamics change leg mechanics for an unexpected surface during human hopping. *J. Appl. Physiol.* **97**, 1313-1322.

Müller, R. and Blickhan, R. (2010). Running on uneven ground: leg adjustments to altered ground level. *Hum. Mov. Sci.* **29**, 578-589.

Müller, R., Grimmer, S. and Blickhan, R. (2010). Running on uneven ground: leg adjustments by muscle pre-activation control. *Hum. Mov. Sci.* **29**, 299-310.

Pakan, J. M. P. and Wylie, D. R. W. (2006). Two optic flow pathways from the pretectal nucleus lentiformis mesencephali to the cerebellum in pigeons (*Columba livia*). *J. Comp. Neurol.* **499**, 732-744.

Patla, A. E. (1997). Understanding the roles of vision in the control of human locomotion. *Gait Posture* **5**, 54-69.

Patla, A. E., Robinson, C., Samways, M. and Armstrong, C. J. (1989). Visual control of step length during overground locomotion: task-specific modulation of the locomotor synergy. *J. Exp. Psychol.* **15**, 603-617.

Rice, W. R. (1989). Analyzing tables of statistical tests. *Evolution* **43**, 223-225.

Schaeffel, F., Hagel, G., Eikermann, T. and Collett, T. (1994). Lower-field myopia and astigmatism in amphibians and chickens. *J. Opt. Soc. Am. A* **11**, 487-495.

Schmitt, J. and Clark, J. (2009). Modeling posture-dependent leg actuation in sagittal plane locomotion. *Bioinspir. Biomim.* **4**, 046005.

Seipel, J. E. and Holmes, P. J. (2007). A simple model for clock-actuated legged locomotion. *Reg. Chaotic Dyn.* **12**, 502-520.

Seipel, J. E., Holmes, P. J. and Full, R. J. (2004). Dynamics and stability of insect locomotion: a hexapedal model for horizontal plane motions. *Biol. Cybern.* **91**, 76-90.

Seyfarth, A., Geyer, H., Gunther, M. and Blickhan, R. (2002). A movement criterion for running. *J. Biomech.* **35**, 649-655.

Seyfarth, A., Geyer, H. and Herr, H. (2003). Swing-leg retraction: a simple control model for stable running. *J. Exp. Biol.* **206**, 2547-2555.

Seyfarth, A., Geyer, H., Blickhan, R., Lipfert, S., Rummel, J., Minekawa, Y. and Iida, F. (2006). Running and walking with compliant legs. In *Fast Motions in Biomechanics and Robotics* (ed. M. Diehl and K. Mombaur), pp. 383-401. Heidelberg: Springer-Verlag.

Smith, J. L., Chung, S. H. and Zernicke, R. F. (1993). Gait-related motor patterns and hindlimb kinetics for the cat trot and gallop. *Exp. Brain Res.* **94**, 308-322.

Sokal, R. R. and Rohlf, F. J. (ed.) (1995). Multiple and curvilinear regression. In *Biometry: The Principles and Practice of Statistics in Biological Research*, 3rd edn, pp. 634-649. New York, Oxford: Freeman.

Sponberg, S. and Full, R. J. (2008). Neuromechanical response of musculo-skeletal structures in cockroaches during rapid running on rough terrain. *J. Exp. Biol.* **211**, 433-446.

Wilkie, R., Kountouriotis, G., Merat, N. and Wann, J. (2010). Using vision to control locomotion: looking where you want to go. *Exp. Brain Res.* **204**, 539-547.